Approximating the Conformal Map of Elongated Quadrilaterals by Domain Decomposition

M.I. Falcão, N. Papamichael and N.S. Stylianopoulos

April 2, 2000

Abstract

Let $Q := \{\Omega; z_1, z_2, z_3, z_4\}$ be a quadrilateral consisting of a Jordan domain Ω and four points z_1, z_2, z_3, z_4, in counterclockwise order on $\partial\Omega$ and let $m(Q)$ be the conformal module of Q. Then Q is conformally equivalent to the rectangular quadrilateral $\{R_{m(Q)}; 0, 1, 1 + im(Q), im(Q)\}$, where $R_{m(Q)} := \{(\xi, \eta) : 0 < \xi < 1,\ 0 < \eta < m(Q)\}$, in the sense that there exists a unique conformal map $f : \Omega \to R_{m(Q)}$ that takes the four points z_1, z_2, z_3, z_4, respectively onto the four vertices 0, 1, $1 + im(Q)$, $im(Q)$ of $R_{m(Q)}$. In this paper we consider the use of a domain decomposition method (DDM) for computing approximations to the conformal map f, in cases where the quadrilateral Q is "long". The method has been studied already but, mainly, in connection with the computation of $m(Q)$. Here we consider certain recent results of Laugesen [12], for the DDM approximation of the conformal map $f : \Omega \to R_{m(Q)}$ associated with a special class of quadrilaterals (viz. quadrilaterals whose two non-adjacent boundary segments (z_2, z_3) and (z_4, z_1) are parallel straight lines) and seek to extend these results to more general quadrilaterals. By making use of the available DDM theory for conformal modules, we show that the corresponding theory for f can, indeed, be extended to a much wider class of quadrilaterals than those considered by Laugesen.

AMS classification: 30C30, 65E05.

Key words Numerical conformal mapping, Quadrilaterals, Domain decomposition.

1 Introduction

Let $Q := \{\Omega; z_1, z_2, z_3, z_4\}$ be a quadrilateral consisting of a Jordan domain Ω and four points z_1, z_2, z_3, z_4 in counterclockwise order on $\partial\Omega$ and let $m(Q)$ be the conformal module of Q. Also, let $R_{m(Q)}$ denote a rectangle of base 1 and height $m(Q)$, i.e.

$$R_{m(Q)} := \{(\xi, \eta) : 0 < \xi < 1,\ 0 < \eta < m(Q)\}.$$

Then, Q is conformally equivalent to the rectangular quadrilateral

$$\{R_{m(Q)}; 0, 1, 1 + im(Q), im(Q)\},$$

in the sense that there exists a unique conformal map $f : \Omega \to R_{m(Q)}$ that takes the four points z_1, z_2, z_3, z_4, respectively onto the four vertices 0, 1, $1 + im(Q)$, $im(Q)$ of $R_{m(Q)}$.

This paper is concerned with the study of a domain decomposition method (DDM) for computing approximations to the conformal module $m(Q)$ and the associated conformal map $f : \Omega \to R_{m(Q)}$, in cases where the quadrilateral Q is long. The method is based on the following three steps:

(i) Decomposing the original quadrilateral $Q := \{\Omega; z_1, z_2, z_3, z_4\}$(by means of appropriate crosscuts l_j; $j = 1, 2, \ldots$) into two or more component quadrilaterals Q_j; $j = 1, 2, \ldots$; see e.g. Figure 1.1.

(ii) Approximating the conformal module $m(Q)$ of the original quadrilateral by the sum $\sum_j m(Q_j)$ of the conformal modules of the component quadrilaterals. (Note that

$$m(Q) \geq \sum_j m(Q_j) \tag{1.1}$$

and equality occurs only when the images of all the crosscuts l_j under the conformal map $f : \Omega \to R_{m(Q)}$ are straight lines parallel to the real axis. This follows from the well-known composition law for modules of curve families; see e.g. [1, pp. 54–56] and [9, pp. 437–438].)

(iii) Approximating the conformal map $f : \Omega \to R_{m(Q)}$ of the original domain Ω, by the conformal maps $f_j : \Omega_j \to R_{m(Q_j)}$ of the subdomains Ω_j, where

$$R_{m(Q_1)} := \{(\xi, \eta) : 0 < \xi < 1,\ 0 < \eta < m(Q_1)\}$$

and

$$R_{m(Q_j)} := \{(\xi, \eta) : 0 < \xi < 1,\ \sum_{k=1}^{j-1} m(Q_k) < \eta < \sum_{k=1}^{j} m(Q_k)\},\ j = 2, 3, \ldots .$$

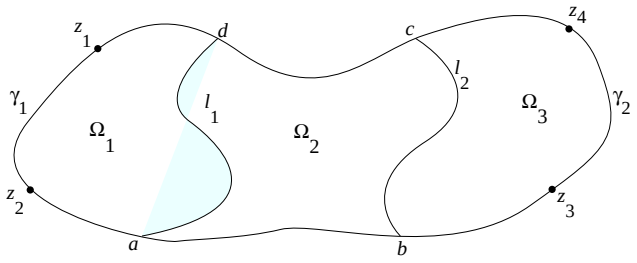

Figure 1.1

The specific objectives for using the above process are as follows:

(a) To overcome the crowding difficulties associated with the problem of computing the conformal maps of long quadrilaterals, i.e. the difficulties associated with the conventional approach of seeking to determine $m(Q)$ and $f : \Omega \to R_{m(Q)}$ by going via the unit disc or the half plane (see e.g. [13, §3.1] and [17, §1]).

(b) To take advantage of the fact that in many applications (for example VLSI applications), a complicated original quadrilateral Q can be decomposed into very simple components Q_j.

The DDM was introduced by two of the present authors (N.P. and N.S.S.) in [14], [15], for the purpose of computing the conformal modules and associated conformal maps of a special class of quadrilaterals, viz. quadrilaterals where: (a) the defining domain Ω is bounded by two parallel straight lines

and two Jordan arcs; (b) the points z_1, z_2, z_3, z_4 are the four corners where the two boundary arcs meet the two parallel straight lines. For the same special class of quadrilaterals, the method was also studied by Gaier and Hayman [5], [6], in connection with the computation of conformal modules, and more recently by Laugesen [12], in connection with the determination of the conformal maps. These three papers contain several important results that enhance considerably the associated DDM theory. In particular, the results of Gaier and Hayman provided the necessary tools for extending the application of the DDM to the computation of the conformal modules of a much wider class of quadrilaterals than that considered initially in [14] and [15] (see [16], [17], [18], [19]). The main purpose of the present paper is to investigate the possibility of extending the DDM theory of Laugesen [12], for the conformal map $f : \Omega \to R_{m(Q)}$, to more general quadrilaterals than those having the special form mentioned above.

The paper is organised as follows:

In Section 2 we present a number of preliminary results that are needed for our work in Section 3.

Section 3 contains the main results of the paper. Here, by making use of the theory given in Section 2, we show that Laugesen's DDM theory for the mapping function f can indeed be extended to a much wider class of quadrilaterals than those considered in [12].

Finally, in Section 4 we present several numerical examples illustrating the application of the DDM results obtained in Section 3.

In presenting our results we shall adopt throughout the notations used in [16], [17], [18]. That is:

- Ω and $Q := \{\Omega; z_1, z_2, z_3, z_4\}$ will denote respectively the original domain and corresponding quadrilateral.

- $\Omega_1, \Omega_2, \ldots$ and $Q_1, Q_2, \ldots$, will denote respectively the "principal" subdomains and corresponding quadrilaterals of the decomposition under consideration.

- The additional subdomains and associated quadrilaterals that arise when the decomposition of Q involves more than one crosscut will be denoted by using (in an obvious manner) a multisubscript notation.

For example, the five component quadrilaterals of the decomposition illustrated in Figure 1.1 are:

$$Q_1 := \{\Omega_1; z_1, z_2, a, d\}, \quad Q_2 := \{\Omega_2; d, a, b, c\}, \quad Q_3 := \{\Omega_3; c, b, z_3, z_4\}$$

and

$$Q_{1,2} := \{\Omega_{1,2}; z_1, z_2, b, c\}, \quad Q_{2,3} := \{\Omega_{2,3}; d, a, z_3, z_4\},$$

where

$$\overline{\Omega}_{1,2} := \overline{\Omega}_1 \cup \overline{\Omega}_2, \quad \overline{\Omega}_{2,3} := \overline{\Omega}_2 \cup \overline{\Omega}_3.$$

2 Preliminary results

In this section we present a number of preliminary results that are needed for our work in Section 3. The first of these (Lemma 2.1) is a simple consequence of results given in [12].

Consider a quadrilateral of the form illustrated in Figure 2.1(a), where: (a) the defining domain Ω is bounded by the straight lines $\Re z = 0$, $\Re z = 1$ and $\gamma_1 := \{z : 0 \le \Re z \le 1,\ \Im z = 0\}$ and a Jordan arc γ_2; (b) the four points z_1, z_2, z_3, z_4 are the four corners where γ_1 and γ_2 meet the lines $\Re z = 1$ and $\Re z = 0$.

Consider next the decomposition of Q illustrated in the figure, where the crosscut of subdivision is a Jordan arc γ joining the straight lines $\Re z = 0$ and $\Re z = 1$. Also let $R_{m(Q)}$ and $R_{m(Q_2)}$ denote the rectangles

$$R_{m(Q)} := \{(\xi, \eta) : 0 < \xi < 1,\ 0 < \eta < m(Q)\}$$

and

$$R_{m(Q_2)} := \{(\xi, \eta) : 0 < \xi < 1,\ m(Q) - m(Q_2) < \eta < m(Q)\}$$

and let f and f_2 be the associated conformal maps

$$f : \Omega \to R_{m(Q)} \qquad \text{and} \qquad f_2 : \Omega_2 \to R_{m(Q_2)}. \tag{2.1}$$

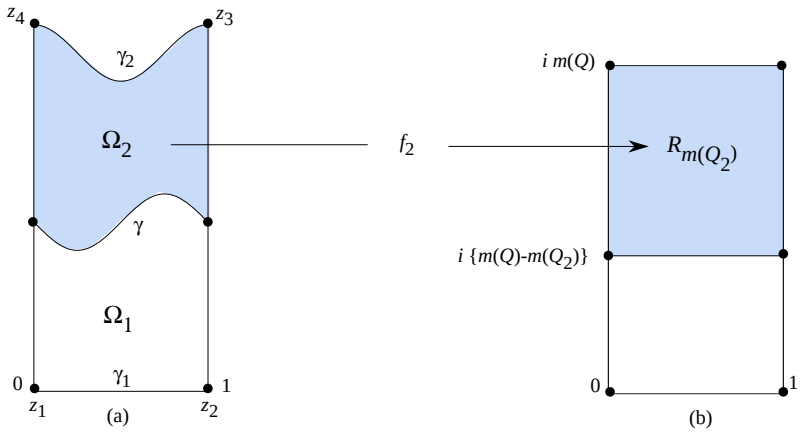

Figure 2.1

Lemma 2.1 *With reference to Figure 2.1 and the notations introduced above,*

$$\max_{z\in\gamma_2} |f(z) - f_2(z)| \le 1.28e^{-\pi m(Q_2)}, \tag{2.2}$$

$$\max_{z\in\gamma_1} |f(z) - z| \le 1.60e^{-\pi m(Q)}, \tag{2.3}$$

and

$$\max_{z\in\overline{\Omega}_1} |f(z) - z| = \max_{z\in\gamma} |f(z) - z| \le 6.40e^{-\pi m(Q_2)}, \tag{2.4}$$

provided that $m(Q_2) \ge 3$. *If, in addition, the crosscut* γ *is a straight line parallel to the real axis, then*

$$\max_{z\in\gamma_2} |f(z) - f_2(z)| \le 2.57e^{-2\pi m(Q_2)}, \tag{2.5}$$

$$\max_{z\in\gamma_1} |f(z) - z| \le 2.04e^{-\pi m(Q)}, \tag{2.6}$$

and

$$\max_{z\in\overline{\Omega}_1} |f(z) - z| = \max_{z\in\gamma} |f(z) - z| \le 2.04e^{-\pi m(Q_2)}, \tag{2.7}$$

provided that $m(Q_2) \ge 1$.

Proof. Of the above, Estimates (2.2) and (2.5) can be concluded trivially from the analysis of Laugesen [12], by noting that in our case γ_2 and γ

are Jordan arcs and applying Estimate (6.6) of [12, p. 550] to each of the exponential mappings associated with the conformal maps f and f_2. The remaining estimates can be obtained as follows:

The transformation

$$z \to Z := \exp(i\pi z),$$

maps conformally Ω onto the upper half of a symmetric doubly-connected domain G which is bounded externally by the unit circle and internally by a Jordan curve Γ surrounding the origin. Let $1/r$ be the conformal modulus of G and let g be the function that maps conformally G onto the circular annulus $A := \{W : r < |W| < 1\}$. Then g is related to the mapping function $f : \Omega \to R_{m(Q)}$ by means of

$$g\{\exp(i\pi z)\} = \exp\{i\pi f(z)\}, \tag{2.8}$$

and

$$r = \exp\{-\pi m(Q)\}. \tag{2.9}$$

Next, apply the so-called 5r-theorem of Laugesen [12, p. 535] to the mapping function $g^{-1} : A \to G$. Then, by adapting the analysis of Laugesen [12, p. 550] to our case and noting that the inner boundary Γ of G is a Jordan curve, we find that for any ρ, $e^{-\pi h} \le \rho \le 1$, where $h := \max\{\Im z,\ z \in \gamma\}$,

$$\max_{|Z|=\rho} |\log g(Z) - \log Z| \le \frac{5r}{\rho - 5r}, \tag{2.10}$$

provided $r < \rho/5$. From this it follows easily that

$$\max_{z\in\gamma_1} |f(z) - z| \le \frac{5r}{1 - 5r}, \tag{2.11}$$

provided $r \le 1/5$, and

$$\max_{z\in\overline{\Omega}_1} |f(z) - z| = \max_{z\in\gamma} |f(z) - z| \le \frac{5e^{-\pi\{m(Q)-h\}}}{\pi(1 - 5e^{-\pi\{m(Q)-h\}})}, \tag{2.12}$$

provided $m(Q) - h \ge (\log 5)/\pi = 0.512\cdots$. Estimates (2.3) and (2.6) then follow at once from (2.11), because $m(Q) \ge m(Q_2)$. Further, (2.12) with $m(Q) - h \ge 1$ gives

$$\max_{z\in\overline{\Omega}_1} |f(z) - z| \le 2.04e^{-\pi\{m(Q)-h\}},$$

and (2.7) follows from this, because when γ is a straight line, then

$$m(Q) \geq m(Q_2) + h.$$

Finally, to obtain Estimate (2.4) we make use of the following:
(i) The double inequality

$$h_2 \leq m(Q_2) \leq h_2 + 1, \tag{2.13}$$

where h_2 is the distance of the crosscut γ from the arc γ_2; see [8, pp. 35–37].
(ii) The following two results of Gaier and Hayman (see [6, Thms 1, 4] and [16, Thm 2.1]):

- $$|m(Q_2) - h_2 - \frac{1}{\pi}\log r_1 - \frac{1}{\pi}\log r_2| \leq 0.381 e^{-\pi h_2}, \tag{2.14}$$

  provided $h_2 \geq 2$, where r_1 and r_2 are the so-called exponential radii of the arcs γ and $\overline{\gamma_2}$, respectively. (Here $\overline{\gamma_2}$ denotes the reflection of the arc γ_2 in the real axis.)

- Let $\widehat{Q}$ be the quadrilateral

  $$\widehat{Q} := \{\widehat{\Omega}; ih, 1 + ih, z_3, z_4\},$$

  where $\widehat{\Omega} = \Omega_2 \cap \{z : \Im z > h\}$. Then,

  $$-\frac{1}{2}0.381 e^{-2\pi h_2} < m(\widehat{Q}) - h_2 - \frac{1}{\pi}\log r_2 \leq 0, \tag{2.15}$$

  provided $h_2 \geq 1$.

(iii) The two inequalities

$$m(Q) \geq m(\widehat{Q}) + h \qquad \text{and} \qquad r_1 \leq 4, \tag{2.16}$$

which result, respectively, from the composition law (1.1) and Koebe's $\frac{1}{4}$-theorem.

Estimate (2.4) follows from (2.12), because (2.13)–(2.16) imply that

$$m(Q) - h > m(Q_2) - 0.441\ 983\ 4. \qquad \blacksquare$$

Let Q be the quadrilateral $Q := \{R_H; 0, 1, 1 + iH, iH\}$, where

$$R_H := \{(\xi, \eta) : 0 < \xi < 1,\ 0 < \eta < H\},$$

and consider a decomposition of Q by means of two Jordan arcs l_1 and l_2 as illustrated in Figure 2.2. With the usual notations, let $Q_{1,2}$, Q_2 and $Q_{2,3}$ be the three quadrilaterals that are defined respectively by the subdomains $\Omega_{1,2}$, Ω_2, and $\Omega_{2,3}$ and let $R_{m(Q_{1,2})}$, $R_{m(Q_2)}$ and $R_{m(Q_{2,3})}$ be the corresponding conformally equivalent rectangles

$$R_{m(Q_{1,2})} := \{(\xi, \eta) : 0 < \xi < 1,\ 0 < \eta < m(Q_{1,2})\}, \tag{2.17}$$

$$R_{m(Q_2)} := \{(\xi, \eta) : 0 < \xi < 1,\ m(Q_{1,2}) - m(Q_2) < \eta < m(Q_{1,2})\} \tag{2.18}$$

and

$$R_{m(Q_{2,3})} := \{(\xi, \eta) : 0 < \xi < 1,\ H - m(Q_{2,3}) < \eta < H\}. \tag{2.19}$$

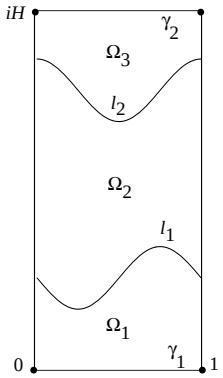

Figure 2.2

Finally, let $f_{1,2}$, f_2 and $f_{2,3}$ denote the associated conformal maps (see Figure 2.3),

$$f_{1,2} : \Omega_{1,2} \to R_{m(Q_{1,2})}, \quad f_2 : \Omega_2 \to R_{m(Q_2)}, \quad f_{2,3} : \Omega_{2,3} \to R_{m(Q_{2,3})},$$

and consider the transformation $T : R_H \to R_H$ defined by

$$T(\zeta) := \begin{cases} f_{2,3}(\zeta), \text{ for } \zeta \in \Omega_3, \\ f_{1,2}(\zeta) + f_{2,3}(\zeta) - f_2(\zeta), \text{ for } \zeta \in \Omega_2, \\ f_{1,2}(\zeta), \text{ for } \zeta \in \Omega_1. \end{cases} \tag{2.20}$$

The lemma below says that if R_H is "long", then T is close to the identity map.

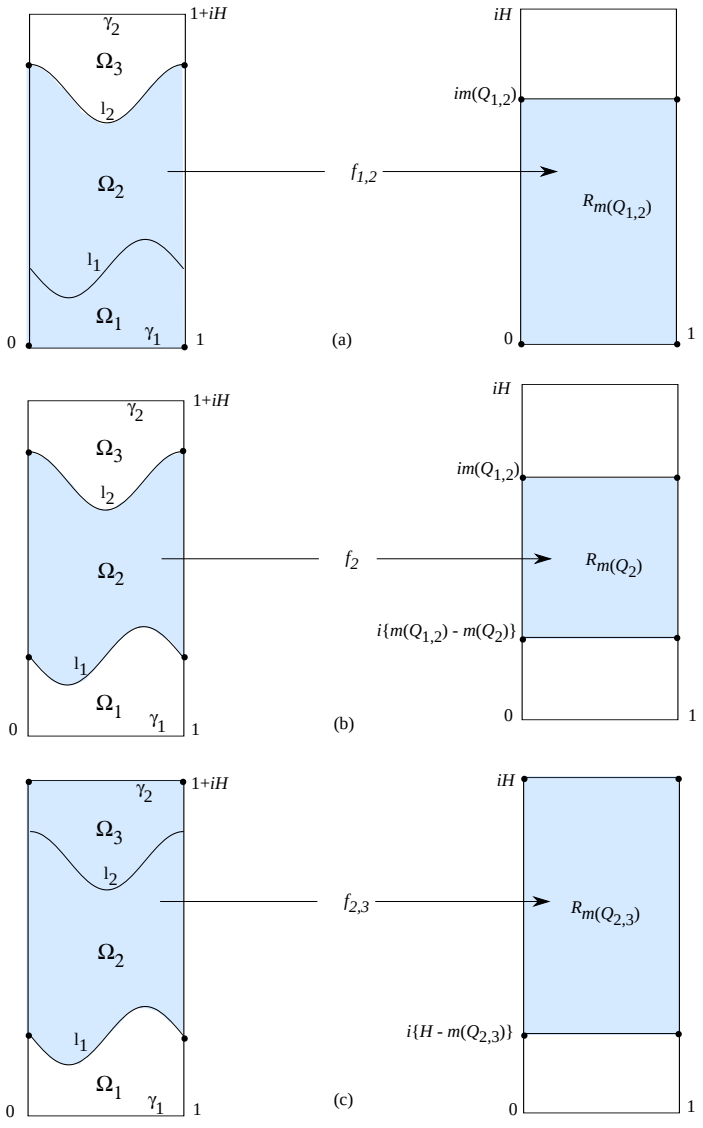

Figure 2.3

Lemma 2.2 *With reference to Figures 2.2 and 2.3 and the notations introduced above,*

$$E_T := \max_{\zeta \in \overline{R}_H} |T(\zeta) - \zeta| \leq 10.39 e^{-\pi m(Q_2)}, \tag{2.21}$$

provided that $m(Q_2) \geq 3$. *If, in addition, the crosscut* l_1 *is a straight line parallel to the real axis (so that* $f_{2,3}(\zeta) = \zeta$*), then*

$$E_T \leq 4.08 e^{-\pi m(Q_2)}, \tag{2.22}$$

provided that $m(Q_2) \geq 1$.

Proof. From (2.4),

$$E_T = \max\{\max_{\zeta \in l_1} |f_{1,2}(\zeta) - \zeta|,\ \max_{\zeta \in \overline{\Omega}_2} |T(\zeta) - \zeta|,\ \max_{\zeta \in l_2} |f_{2,3}(\zeta) - \zeta|\}, \tag{2.23}$$

where

$$\max_{\zeta \in l_1} |f_{1,2}(\zeta) - \zeta| \leq 6.40 e^{-\pi m(Q_2)} \tag{2.24}$$

and

$$\max_{\zeta \in l_2} |f_{2,3}(\zeta) - \zeta| \leq 6.40 e^{-\pi m(Q_2)}, \tag{2.25}$$

provided $m(Q_2) \geq 3$. Further, the function $T(\zeta) - \zeta$ is analytic in Ω_2, continuous on $\overline{\Omega}_2$ and can be extended (by means of the Schwarz reflection principle) to a periodic function, with period 2, in the infinite domain obtained by repeatedly reflecting Ω_2 across its straight line boundary segments (see e.g. [7, p. 273]). Therefore, from the maximum modulus principle,

$$\max_{\zeta \in \overline{\Omega}_2} |T(\zeta) - \zeta| = \max\{E_{l_1}, E_{l_2}\}, \tag{2.26}$$

where

$$E_{l_1} := \max_{\zeta \in l_1} |f_{1,2}(\zeta) + f_{2,3}(\zeta) - f_2(\zeta) - \zeta|$$

and

$$E_{l_2} := \max_{\zeta \in l_2} |f_{1,2}(\zeta) + f_{2,3}(\zeta) - f_2(\zeta) - \zeta|.$$

Next, if $m(Q_2) \geq 3$, then from (2.2) and (2.4) we have that

$$\begin{aligned} E_{l_2} &\leq \max_{\zeta \in l_2} |f_{1,2}(\zeta) - f_2(\zeta)| + \max_{\zeta \in l_2} |f_{2,3}(\zeta) - \zeta| \\ &\leq 1.28 e^{-\pi m(Q_2)} + 6.40 e^{-\pi m(Q_2)} = 7.68 e^{-\pi m(Q_2)}, \end{aligned} \tag{2.27}$$

and

$$\begin{aligned} E_{l_1} &\leq \max_{\zeta\in l_1} |f_{2,3}(\zeta) - f_2(\zeta) - i\varepsilon_m| + |\varepsilon_m| + \max_{\zeta\in l_1} |f_{1,2}(\zeta) - \zeta| \\ &\leq 1.28e^{-\pi m(Q_2)} + |\varepsilon_m| + 6.40e^{-\pi m(Q_2)}. \end{aligned}$$

(The quantity

$$\varepsilon_m := H - \{m(Q_{1,2}) + m(Q_{2,3}) - m(Q_2)\}$$

was introduced in the last estimate, because the function $f_{2,3}$ maps the domain $\Omega_{2,3}$ onto the rectangle $R_{m(Q_{2,3})}$ whose lower side is at a distance $H - m(Q_{2,3})$, rather than $m(Q_{1,2}) - m(Q_2)$, from the real axis.) Thus, since from Theorem 2.4 of [19]

$$|\varepsilon_m| \leq 2.71e^{-\pi m(Q_2)},$$

we have that

$$E_{l_1} \leq 10.39e^{-\pi m(Q_2)}. \tag{2.28}$$

The required result (2.21) follows from (2.23), by comparing the estimates (2.24), (2.25), (2.27) and (2.28).

If l_1 is a straight line parallel to the real axis and $m(Q_2) \geq 1$, then from (2.7),

$$\max_{\zeta\in l_1} |f_{1,2}(\zeta) - \zeta| \leq 2.04e^{-\pi m(Q_2)} \tag{2.29}$$

and

$$\max_{\zeta\in l_2} |f_{2,3}(\zeta) - \zeta| \leq 2.04e^{-\pi m(Q_2)}. \tag{2.30}$$

Also, since in this case $f_{2,3}(\zeta) = \zeta$, (2.5) gives

$$E_{l_2} = \max_{\zeta\in l_2} |f_{1,2}(\zeta) - f_2(\zeta)| \leq 2.57e^{-2\pi m(Q_2)}. \tag{2.31}$$

Finally, from (2.6),

$$\max_{\zeta\in l_1} |f_2(\zeta) - \zeta| \leq 2.04e^{-2\pi m(Q_2)},$$

and hence

$$E_{l_1} \leq \max_{\zeta\in l_1} |f_2(\zeta) - \zeta| + \max_{\zeta\in l_1} |f_{1,2}(\zeta) - \zeta| \leq 4.08e^{-\pi m(Q_2)}. \tag{2.32}$$

The required result (2.22) follows from (2.23), by comparing the estimates (2.29), (2.30), (2.31) and (2.32). ■

Consider now a general quadrilateral $Q := \{\Omega; z_1, z_2, z_3, z_4\}$ decomposed as shown in Figure 2.4(a). Let f be the conformal map

$$f : \Omega \to R_{m(Q)} := \{(\xi, \eta) : 0 < \xi < 1,\ 0 < \eta < m(Q)\},$$

let $R_{m(Q_{1,2})}$, $R_{m(Q_2)}$, $R_{m(Q_{2,3})}$ denote the rectangles (2.17)–(2.19), with $H = m(Q)$ for $R_{m(Q_{2,3})}$, and let $f_{1,2}$, f_2 and $f_{2,3}$ denote the conformal maps,

$$f_{1,2} : \Omega_{1,2} \to R_{m(Q_{1,2})}, \quad f_2 : \Omega_2 \to R_{m(Q_2)} \quad \text{and} \quad f_{2,3} : \Omega_{2,3} \to R_{m(Q_{2,3})}.$$

Also, let $\tilde{f}$ denote the following DDM approximation to f:

$$\tilde{f}(z) := \begin{cases} f_{2,3}(z), \text{ for } z \in \Omega_3, \\ f_{1,2}(z) + f_{2,3}(z) - f_2(z), \text{ for } z \in \Omega_2, \\ f_{1,2}(z), \text{ for } z \in \Omega_1. \end{cases} \tag{2.33}$$

The theorem below may be regarded as the extension of the conformal module Theorem 2.5 of [19], to the case of the conformal map f.

Theorem 2.1 *With reference to Figure 2.4(a), let $\tilde{f}$ be the DDM approximation (2.33) to the conformal map $f : \Omega \to R_{m(Q)}$. Then*

$$E_f := \max_{z \in \overline{\Omega}} |f(z) - \tilde{f}(z)| \leq 10.39 e^{-\pi m(Q_2)}, \tag{2.34}$$

provided that $m(Q_2) \geq 3$. If, in addition, the image of the crosscut l_1 under the conformal map f is a straight line parallel to the real axis, then

$$E_f \leq 4.08 e^{-\pi m(Q_2)}, \tag{2.35}$$

provided that $m(Q_2) \geq 1$.

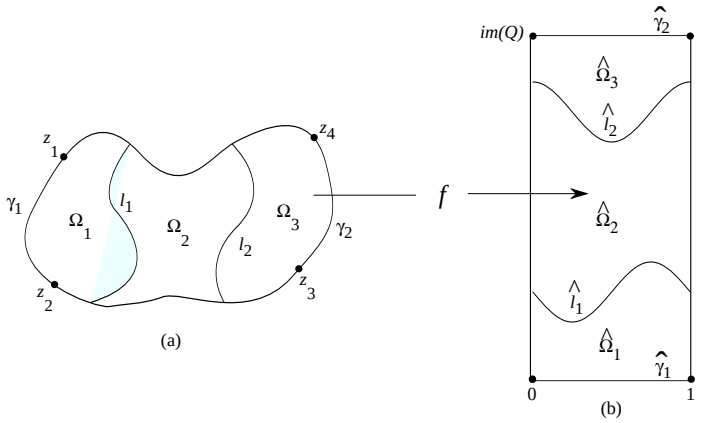

Figure 2.4

Proof. Let $\widehat{\Omega}_1$, $\widehat{\Omega}_2$, $\widehat{\Omega}_3$, $\hat{l}_1$, $\hat{l}_2$, $\hat{\gamma}_1$ and $\hat{\gamma}_2$ denote respectively the images under the conformal map f of Ω_1, Ω_2, Ω_3, l_1, l_2, $\gamma_1 := \widehat{z_1, z_2}$ and $\gamma_2 := \widehat{z_3, z_4}$ (see Figure 2.4), and denote by $\hat{f}_{1,2}$, $\hat{f}_2$ and $\hat{f}_{2,3}$ the conformal maps,

$$\hat{f}_{1,2} : \widehat{\Omega}_{1,2} \to R_{m(Q_{1,2})}, \quad \hat{f}_2 : \widehat{\Omega}_2 \to R_{m(Q_2)} \quad \text{and} \quad \hat{f}_{2,3} : \widehat{\Omega}_{2,3} \to R_{m(Q_{2,3})}.$$

Then,

$$f_{1,2}(z) = \hat{f}_{1,2}(f(z)), \text{ for } z \in \Omega_{1,2}, \quad f_2(z) = \hat{f}_2(f(z)), \text{ for } z \in \Omega_2,$$

and

$$f_{2,3}(z) = \hat{f}_{2,3}(f(z)), \quad \text{for } z \in \Omega_{2,3}.$$

Next, let

$$T(\zeta) := \begin{cases} \hat{f}_{2,3}(\zeta), \text{ for } \zeta \in \widehat{\Omega}_3, \\ \hat{f}_{1,2}(\zeta) + \hat{f}_{2,3}(\zeta) - \hat{f}_2(\zeta), \text{ for } \zeta \in \widehat{\Omega}_2, \\ \hat{f}_{1,2}(\zeta), \text{ for } \zeta \in \widehat{\Omega}_1, \end{cases}$$

and observe that for any $z \in \Omega$, $\tilde{f}(z) = T(\zeta)$, where $\zeta = f(z)$. Thus,

$$E_f = \max_{\zeta \in \overline{R}_{m(Q)}} |T(\zeta) - \zeta|,$$

and the required results follow at once from Lemma 2.2. ■

Remark 2.1 With reference to Theorem 2.1, the following estimates hold:

$$\max_{z\in\gamma_1} |f(z) - f_{1,2}(z)| \leq 1.60 e^{-\pi m(Q_{1,2})} \tag{2.36}$$

and

$$\max_{z\in\gamma_2} |f(z) - f_{2,3}(z)| \leq 1.60 e^{-\pi m(Q_{2,3})}, \tag{2.37}$$

provided that $m(Q_2) \geq 3$. This can be seen by observing that

$$\max_{z\in\gamma_1} |f(z) - f_{1,2}(z)| = \max_{\zeta\in\hat{\gamma}_1} |\hat{f}_{1,2}(\zeta) - \zeta|,$$

$$\max_{z\in\gamma_2} |f(z) - f_{2,3}(z)| = \max_{\zeta\in\hat{\gamma}_2} |\hat{f}_{2,3}(\zeta) - \zeta|$$

(see Figure 2.4(b)) and applying Estimate (2.3) to the right hand side of the last two equations.

3 DDM for the conformal map

The results of this section extend the DDM conformal module results of Theorems 2.4 and 2.6 of [19] to the case of the full conformal map.

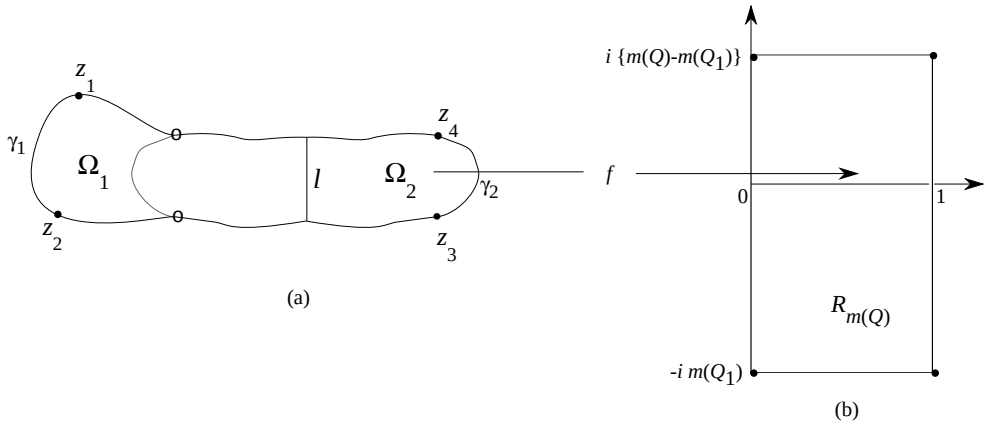

Figure 3.1

Consider a quadrilateral $Q := \{\Omega; z_1, z_2, z_3, z_4\}$ of the form illustrated in Figure 3.1(a), where the defining domain Ω can be decomposed by a straight line crosscut l into Ω_1 and Ω_2, so that Ω_2 is the reflection in l of some

subdomain of Ω_1, as shown in the figure. Let $R_{m(Q)}$, $R_{m(Q_1)}$ and $R_{m(Q_2)}$ be the rectangles

$$R_{m(Q)} := \{(\xi,\eta) : 0 < \xi < 1,\ -m(Q_1) < \eta < m(Q) - m(Q_1)\},$$

$$R_{m(Q_1)} := \{(\xi,\eta) : 0 < \xi < 1,\ -m(Q_1) < \eta < 0\}$$

and

$$R_{m(Q_2)} := \{(\xi,\eta) : 0 < \xi < 1,\ 0 < \eta < m(Q_2)\}$$

and let f_1 and f_2, denote the conformal maps

$$f_1 : \Omega_1 \to R_{m(Q_1)} \quad \text{and} \quad f_2 : \Omega_2 \to R_{m(Q_2)}.$$

The theorem below extends the conformal module Theorem 2.4 of [19] to the case of the conformal map f.

Theorem 3.1 *With reference to Figure 3.1 and the notations introduced above, let $E_f^{\{1\}}$ and $E_f^{\{2\}}$ denote the DDM errors*

$$E_f^{\{1\}} := \max_{z\in\overline{\Omega}_1} |f(z) - f_1(z)| \quad \textit{and} \quad E_f^{\{2\}} := \max_{z\in\overline{\Omega}_2} |f(z) - f_2(z)|. \tag{3.1}$$

Then,

$$E_f^{\{1\}} = \max_{z\in l} |f(z) - f_1(z)| \le 2.04 e^{-\pi m(Q_2)} \tag{3.2}$$

and

$$E_f^{\{2\}} \le 4.08 e^{-\pi m(Q_2)}, \tag{3.3}$$

provided that $m(Q_2) \ge 1$.

Proof. Reflect Ω_1 in l and consider the decomposition of the resulting quadrilateral $Q^* := \{\Omega^*; z_1, z_2, z_3^*, z_4^*\}$ illustrated in Figure 3.2(a). Then the symmetry of Q^* implies that $m(Q^*) = 2m(Q_1)$ and that the image of the crosscut l, under the conformal map

$$g : \Omega^* \to R_{m(Q^*)} := \{(\xi,\eta) : 0 < \xi < 1,\ -m(Q_1) < \eta < m(Q_1)\},$$

is the segment $\widehat{l} := \{(\xi, 0) : 0 \le \xi \le 1\}$ of the real axis.

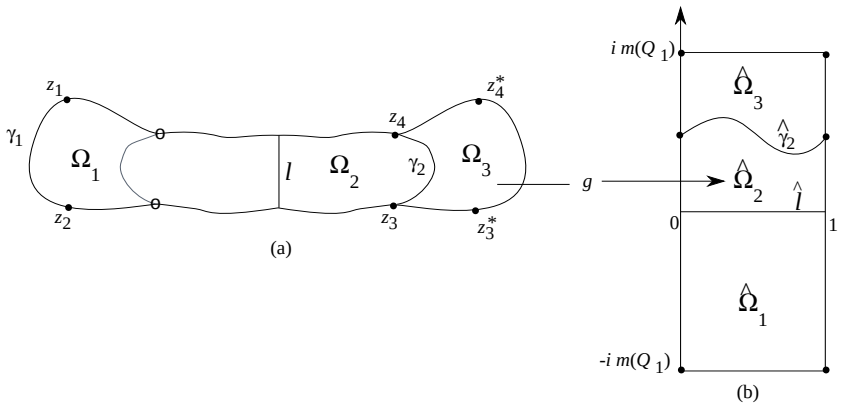

Figure 3.2

Let $\widehat{\Omega}_1$, $\widehat{\Omega}_2$, $\widehat{\Omega}_3$, $\widehat{\gamma}_1$, $\widehat{\gamma}_2$ be the images, under g, of Ω_1, Ω_2, Ω_3, γ_1, γ_2, where $\gamma_1 := \widehat{z_1, z_2}$, $\gamma_2 := \widehat{z_3, z_4}$ (see Figure 3.2), and consider the conformal maps

$$\widehat{g}_1 : \widehat{\Omega}_1 \to R_{m(Q_1)}, \quad \widehat{g}_2 : \widehat{\Omega}_2 \to R_{m(Q_2)} \quad \text{and} \quad \widehat{g}_{1,2} : \widehat{\Omega}_{1,2} \to R_{m(Q)}.$$

Then,

$$f_1(z) = \widehat{g}_1(g(z)),\ z \in \Omega_1, \quad f_2(z) = \widehat{g}_2(g(z)),\ z \in \Omega_2,$$

and

$$f(z) = \widehat{g}_{1,2}(g(z)),\ z \in \Omega.$$

That is,

$$f_1(z) = \widehat{g}_1(\zeta) = \zeta, \quad f_2(z) = \widehat{g}_2(\zeta) \quad \text{and} \quad f(z) = \widehat{g}_{1,2}(\zeta),$$

where $\zeta = g(z)$. Therefore, from (2.7),

$$E_f^{\{1\}} = \max_{\zeta \in \widehat{\overline{\Omega}}_1} |\widehat{g}_{1,2}(\zeta) - \zeta| = \max_{\zeta \in \widehat{l}} |\widehat{g}_{1,2}(\zeta) - \zeta| \tag{3.4}$$

$$= \max_{z \in l} |f(z) - f_1(z)| \le 2.04 e^{-\pi m(Q_2)}. \tag{3.5}$$

Also, by applying to $\widehat{g}_{1,2}(\zeta) - \widehat{g}_2(\zeta)$ the argument used for the function $T(\zeta) - \zeta$ at the beginning of the proof of Lemma 2.2,

$$E_f^{\{2\}} = \max_{\zeta \in \widehat{\overline{\Omega}}_2} |\widehat{g}_{1,2}(\zeta) - \widehat{g}_2(\zeta)| = \max\{E_{\widehat{l}}, E_{\widehat{\gamma}_2}\}, \tag{3.6}$$

where

$$E_{\widehat{l}} := \max_{\zeta\in\widehat{l}} |\widehat{g}_{1,2}(\zeta) - \widehat{g}_2(\zeta)| \quad \text{and} \quad E_{\widehat{\gamma}_2} := \max_{\zeta\in\widehat{\gamma}_2} |\widehat{g}_{1,2}(\zeta) - \widehat{g}_2(\zeta)|.$$

Next, by using (2.6) and (2.7),

$$\begin{aligned} E_{\widehat{l}} &\leq \max_{\zeta\in\widehat{l}} |\widehat{g}_2(\zeta) - \zeta| + \max_{\zeta\in\widehat{l}} |\widehat{g}_{1,2}(\zeta) - \zeta| \\ &\leq 4.08e^{-\pi m(Q_2)}. \end{aligned} \tag{3.7}$$

Also, from (2.5),

$$\begin{aligned} E_{\widehat{\gamma}_2} &\leq \max_{\zeta\in\widehat{\gamma}_2} |\widehat{g}_{1,2}(\zeta) - \widehat{g}_2(\zeta) - i\varepsilon_m| + \varepsilon_m \\ &\leq 2.57e^{-2\pi m(Q_2)} + \varepsilon_m, \end{aligned} \tag{3.8}$$

where the quantity

$$\varepsilon_m := m(Q) - \{m(Q_1) + m(Q_2)\} \tag{3.9}$$

is introduced in (3.8), because the function $\widehat{g}_{1,2}$ maps the domain $\widehat{\Omega}_{1,2}$ onto the rectangle $R_{m(Q)}$ whose upper side is at a distance $m(Q) - m(Q_1)$, rather than $m(Q_2)$, from the real axis. Thus, since from [18, Result 5]

$$0 \leq \varepsilon_m \leq \frac{4}{\pi} e^{-2\pi m(Q_2)},$$

we have that

$$E_{\widehat{\gamma}_2} \leq 3.85e^{-2\pi m(Q_2)}. \tag{3.10}$$

Therefore, from (3.6), (3.7) and (3.10),

$$E_f^{\{2\}} \leq 4.08e^{\pi m(Q_2)}. \qquad \blacksquare$$

Remark 3.1 With reference to Theorem 2.1, the following estimates hold:

$$\max_{z\in\gamma_1} |f(z) - f_1(z)| \leq 2.04e^{-\pi m(Q)} \tag{3.11}$$

and

$$\max_{z\in\gamma_2} |f(z) - f_2(z)| \leq 3.85e^{-2\pi m(Q_2)}, \tag{3.12}$$

provided that $m(Q_2) \geq 1$. The above estimates follow at once from (2.6) and (3.10), because

$$\max_{z \in \gamma_1} |f(z) - f_1(z)| = \max_{\zeta \in \widehat{\gamma}_1} |\widehat{g}_{1,2}(\zeta) - \zeta|$$

and

$$\max_{z \in \gamma_2} |f(z) - f_2(z)| = \max_{\zeta \in \widehat{\gamma}_2} |\widehat{g}_{1,2}(\zeta) - \widehat{g}_2(\zeta)| =: E_{\widehat{\gamma}_2}.$$

Consider now a quadrilateral $Q := \{\Omega; z_1, z_2, z_3, z_4\}$ of the form illustrated in Figure 3.3(a), where the defining domain Ω can be decomposed by means of a straight line crosscut l and two other crosscuts l_1 and l_2 into four subdomains Ω_1, Ω_2, Ω_3 and Ω_4, so that Ω_3 is the reflection in l of Ω_2. Let

$$R_{m(Q)} := \{(\xi, \eta) : 0 < \xi < 1,\ -m(Q_{1,2}) < \eta < m(Q) - m(Q_{1,2})\},$$

$$R_{m(Q_{1,2})} := \{(\xi, \eta) : 0 < \xi < 1,\ -m(Q_{1,2}) < \eta < 0\},$$

$$R_{m(Q_{3,4})} := \{(\xi, \eta) : 0 < \xi < 1,\ 0 < \eta < m(Q_{3,4})\}$$

and denote by f the conformal map $f : \Omega \to R_{m(Q)}$ and by $\tilde{f}$ the following DDM approximation to f:

$$\tilde{f}(z) := \begin{cases} f_{3,4}(z) : \Omega_{3,4} \to R_{m(Q_{3,4})}, \text{ for } z \in \Omega_{3,4}, \\ \\ f_{1,2}(z) : \Omega_{1,2} \to R_{m(Q_{1,2})}, \text{ for } z \in \Omega_{1,2}. \end{cases} \tag{3.13}$$

The theorem below extends the conformal module Theorem 2.6 of [19] to the case of the full conformal map f.

Theorem 3.2 *With reference to Figure 3.3 and the notations introduced above,*

$$E_f := \max_{z \in \overline{\Omega}} |f(z) - \tilde{f}(z)| \leq 6.17 e^{-\pi m(Q_2)}, \tag{3.14}$$

provided that $m(Q_2) \geq 1.5$.

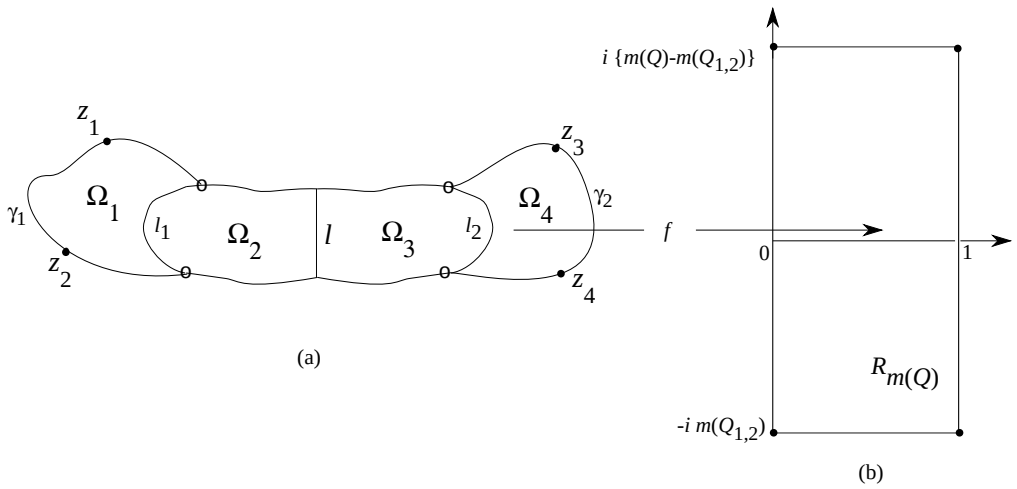

Figure 3.3

Proof. Recall that

$$f : \Omega \to R_{m(Q)} := \{(\xi, \eta) : 0 < \xi < 1,\ -m(Q_{1,2}) < \eta < m(Q) - m(Q_{1,2})\},$$

let

$$R_{m(Q_{1,2,3})} := \{(\xi, \eta) : 0 < \xi < 1,\ -m(Q_{1,2}) < \eta < m(Q_{1,2,3}) - m(Q_{1,2})\},$$

$$R_{m(Q_{2,3})} := \{(\xi, \eta) : 0 < \xi < 1,\ m(Q_{1,2,3}) - m(Q_{1,2}) - m(Q_{2,3}) < \eta < m(Q_{1,2,3}) - m(Q_{1,2})\},$$

$$R_{m(Q_{2,3,4})} := \{(\xi, \eta) : 0 < \xi < 1,\ m(Q) - m(Q_{1,2}) - m(Q_{2,3,4}) < \eta < m(Q) - m(Q_{1,2})\},$$

and consider the transformation

$$g(z) := \begin{cases} f_{2,3,4}(z), \text{ for } z \in \Omega_4, \\ f_{1,2,3}(z) + f_{2,3,4}(z) - f_{2,3}(z), \text{ for } z \in \Omega_{2,3}, \\ f_{1,2,3}(z), \text{ for } z \in \Omega_1, \end{cases}$$

where

$$f_{1,2,3} : \Omega_{1,2,3} \to R_{m(Q_{1,2,3})}, \quad f_{2,3} : \Omega_{2,3} \to R_{m(Q_{2,3})}, \quad f_{2,3,4} : \Omega_{2,3,4} \to R_{m(Q_{2,3,4})}$$

(see Figure 3.4). Then, from Theorem 2.1 (Estimate (2.34)) we have that

$$\max_{z \in \overline{\Omega}} |f(z) - g(z)| \leq 10.39 e^{-2\pi m(Q_2)}, \tag{3.15}$$

provided $m(Q_2) \geq 1.5$. (Note that because of the symmetry $m(Q_{2,3}) = 2m(Q_2)$.)

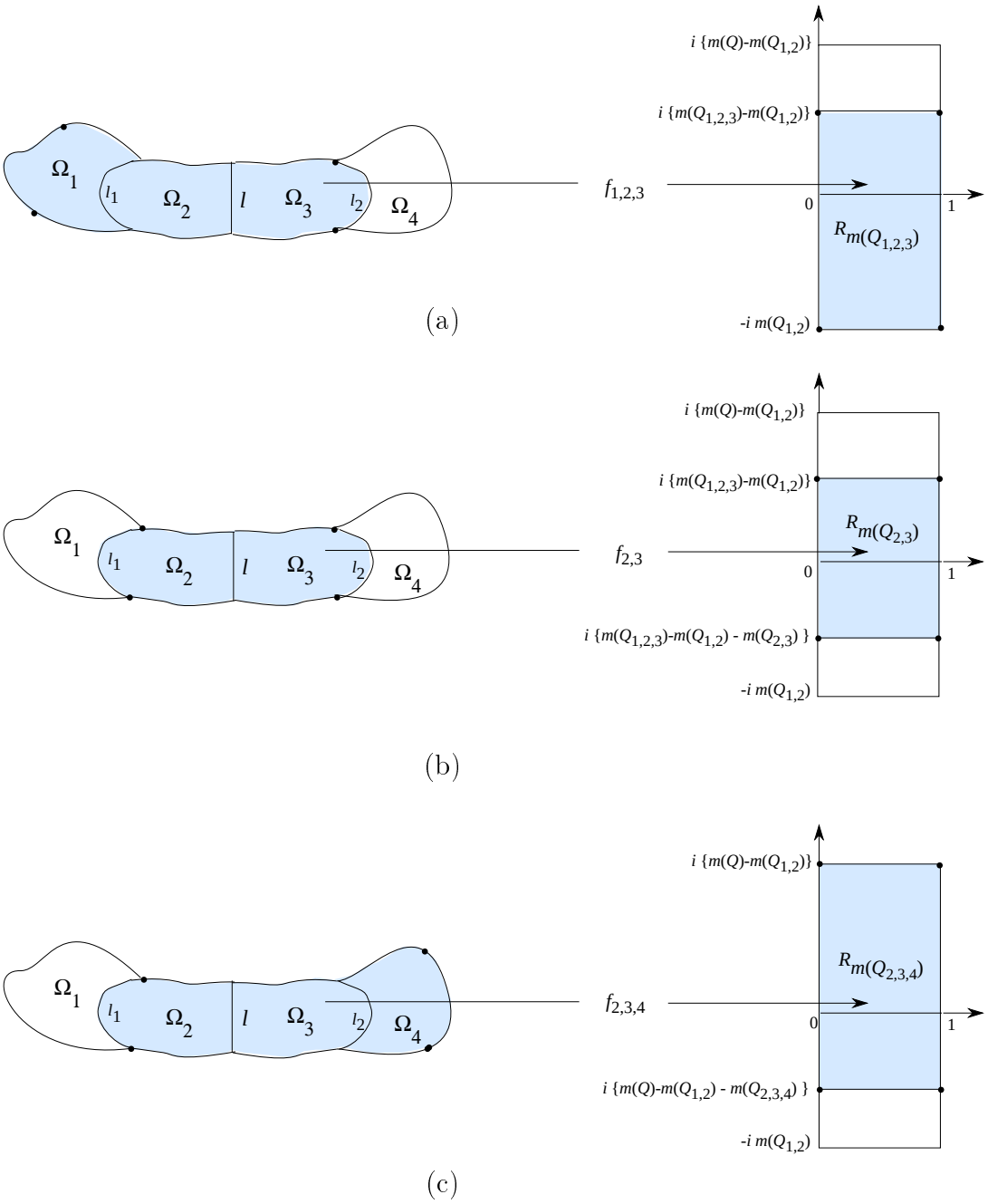

Figure 3.4

Our next objective is to estimate $\max_{z\in\overline{\Omega}}|g(z)-\tilde{f}(z)|$. We do this by estimating separately the errors

$$E_g^{\{j\}} := \max_{z\in\overline{\Omega}_j} |g(z)-\tilde{f}(z)|,\ j=1,2,3,4,$$

as follows:

(i)

$$E_g^{\{1\}} = \max_{z\in\overline{\Omega}_1} |f_{1,2,3}(z)-f_{1,2}(z)|.$$

Therefore, from (3.2),

$$E_g^{\{1\}} \le 2.04e^{-\pi m(Q_2)}, \tag{3.16}$$

provided $m(Q_2)\ge 1$.

(ii)

$$\begin{aligned} E_g^{\{2\}} &= \max_{z\in\overline{\Omega}_2} |f_{1,2,3}(z)+f_{2,3,4}(z)-f_{2,3}(z)-f_{1,2}(z)| \\ &\le \max_{z\in\overline{\Omega}_2} |f_{1,2,3}(z)-f_{1,2}(z)| + \max_{z\in\overline{\Omega}_2} |f_{2,3,4}(z)-f_{2,3}(z)|, \end{aligned} \tag{3.17}$$

where, from (3.2),

$$\max_{z\in\overline{\Omega}_2} |f_{1,2,3}(z)-f_{1,2}(z)| \le 2.04e^{-\pi m(Q_2)}, \tag{3.18}$$

provided $m(Q_2)\ge 1$. Also, if

$$R_{m(Q_2)} := \{(\xi,\eta) : 0<\xi<1,\ H_1<\eta<H_2\},$$

with

$$H_1 := m(Q_{1,2,3})-m(Q_{1,2})-m(Q_{2,3}) \quad \text{and} \quad H_2 := m(Q_{1,2,3})-m(Q_{1,2})-m(Q_3),$$

then, because of the symmetry of $\Omega_{2,3}$,

$$f_{2,3}(z) = f_2(z), \quad z\in\Omega_2,$$

where $f_2:\Omega_2\to R_{m(Q_2)}$. Therefore, if

$$\alpha := m(Q)-\{m(Q_{1,2,3})+m(Q_{2,3,4})-m(Q_{2,3})\},$$

then by using (3.3),

$$\begin{aligned}\max_{z\in\overline{\Omega}_2}|f_{2,3,4}(z)-f_{2,3}(z)| &\leq \max_{z\in\overline{\Omega}_2}|f_{2,3,4}(z)-f_2(z)-i\alpha|+|\alpha| \\ &\leq 4.08e^{-\pi m(Q_2)}+|\alpha|, \end{aligned} \tag{3.19}$$

provided $m(Q_2)\geq 1$. (The quantity α was introduced in the above estimate because the function $f_{2,3,4}$ maps the domain $\Omega_{2,3,4}$ onto the rectangle $R_{m(Q_{2,3,4})}$ whose lower side is at a distance $m(Q)-m(Q_{1,2})-m(Q_{2,3,4})$, rather than $m(Q_{1,2,3})-m(Q_{1,2})-m(Q_{2,3})$, from the real axis; see Figures 3.4(b), (c).) Hence, from (3.17)–(3.19),

$$E_g^{\{2\}}\leq 6.12e^{-\pi m(Q_2)}+|\alpha|, \tag{3.20}$$

provided $m(Q_2)\geq 1$.
(iii)

$$\begin{aligned}E_g^{\{3\}} &= \max_{z\in\overline{\Omega}_3}|f_{1,2,3}(z)+f_{2,3,4}(z)-f_{2,3}(z)-f_{3,4}(z)| \\ &\leq \max_{z\in\overline{\Omega}_3}|f_{1,2,3}(z)-f_{2,3}(z)|+\max_{z\in\overline{\Omega}_3}|f_{2,3,4}(z)-f_{3,4}(z)-i\varepsilon_m|+\varepsilon_m,\end{aligned}$$

where the quantity

$$\varepsilon_m := m(Q)-\{m(Q_{1,2})+m(Q_{3,4})\}$$

is introduced because the function $f_{2,3,4}$ maps the domain $\Omega_{2,3,4}$ onto the rectangle $R_{m(Q_{2,3,4})}$ whose top side is at a distance $m(Q)-m(Q_{1,2})$, rather than $m(Q_{3,4})$, from the real axis; see Figure 3.4(c). Hence, by recognising that

$$f_{2,3}(z)=f_3(z),\quad z\in\Omega_3,$$

with

$$f_3:\Omega_3\to R_{m(Q_3)}:=\{(\xi,\eta):0<\xi<1,\ H_2<\eta<m(Q_{1,2,3})-m(Q_{1,2})\},$$

we obtain from (3.2) and (3.3) that

$$E_g^{\{3\}}\leq 6.12e^{-\pi m(Q_2)}+\varepsilon_m, \tag{3.21}$$

provided $m(Q_2) \geq 1$.

(iv) As in (iii) above, by using (3.2),

$$\begin{aligned} E_g^{\{4\}} &= \max_{z\in\overline{\Omega}_4} |f_{2,3,4}(z) - f_{3,4}(z)| \leq \max_{z\in\overline{\Omega}_4} |f_{2,3,4}(z) - f_{3,4}(z) - i\varepsilon_m| + \varepsilon_m \\ &\leq 2.04e^{-\pi m(Q_2)} + \varepsilon_m, \end{aligned} \tag{3.22}$$

provided $m(Q_2) \geq 1$.

Thus, from (3.15), (3.16) and (3.20)–(3.22),

$$\begin{aligned} E_f &\leq \max_{z\in\overline{\Omega}} |f(z) - g(z)| + \max_{z\in\overline{\Omega}} |g(z) - \tilde{f}(z)|, \\ &\leq 10.39e^{-2\pi m(Q_2)} + \max_{z\in\overline{\Omega}} |g(z) - \tilde{f}(z)|, \end{aligned} \tag{3.23}$$

where

$$|g(z) - \tilde{f}(z)| \leq \begin{cases} 2.04e^{-\pi m(Q_2)}, \text{ for } z \in \overline{\Omega}_1, \\ 6.12e^{-\pi m(Q_2)} + |\alpha|, \text{ for } z \in \overline{\Omega}_2, \\ 6.12e^{-\pi m(Q_2)} + \varepsilon_m, \text{ for } z \in \overline{\Omega}_3, \\ 2.04e^{-\pi m(Q_2)} + \varepsilon_m, \text{ for } z \in \overline{\Omega}_4. \end{cases} \tag{3.24}$$

Finally, if $m(Q_2) \geq 1.5$, then Theorems 2.5 and 2.6 of [19] give,

$$|\alpha| \leq 2.71e^{-2\pi m(Q_2)} \quad \text{and} \quad 0 \leq \varepsilon_m \leq 5.26e^{-2\pi m(Q_2)}. \tag{3.25}$$

These, in conjunction with (3.23) and (3.24), yield the required estimate

$$E_f \leq 6.17e^{-\pi m(Q_2)}. \qquad \blacksquare$$

Remark 3.2 We note the following regarding the various DDM estimates involved in the proof of Theorem 3.2:

(i) Let γ_1, γ_2 denote respectively the sides $\widehat{z_1, z_2}$ and $\widehat{z_3, z_4}$ of the quadrilateral Q (see Figure 3.3). Then, by applying the maximum modulus principle to the functions $f(z) - f_{1,2}(z)$ and $f(z) - f_{3,4}(z)$ (in a way similar to that used for deriving Estimate (3.3) in Theorem 3.1) we find that

$$\max_{z\in\overline{\Omega}_{1,2}} |f(z) - f_{1,2}(z)| = \max\{E_{\gamma_1}, E_l^{\{1\}}\} \tag{3.26}$$

and

$$\max_{z\in\overline{\Omega}_{3,4}} |f(z) - f_{3,4}(z)| = \max\{E_{\gamma_2}, E_l^{\{2\}}\}, \tag{3.27}$$

where,

$$E_{\gamma_1} := \max_{z\in\gamma_1} |f(z) - f_{1,2}(z)|, \quad E_l^{\{1\}} := \max_{z\in l} |f(z) - f_{1,2}(z)| \tag{3.28}$$

and

$$E_{\gamma_2} := \max_{z\in\gamma_2} |f(z) - f_{3,4}(z)|, \quad E_l^{\{2\}} := \max_{z\in l} |f(z) - f_{3,4}(z)|. \tag{3.29}$$

Thus, in order to estimate the full DDM error E_f, it is sufficient to consider the four partial errors E_{γ_1}, $E_l^{\{1\}}$, E_{γ_2} and $E_l^{\{2\}}$. This will be used in Section 4 for the purpose of comparing: (a) the theoretical error estimate (3.14) with the "actual"DDM error (Example 4.1); (b) the DDM approximation $\widetilde{f}$ with approximations obtained by other conformal mapping techniques (Example 4.2).

(ii) For the two boundary errors E_{γ_1} and E_{γ_2}, the following estimates hold:

$$E_{\gamma_1} \le 3.64e^{-\pi m(Q_{1,2,3})} \quad \text{and} \quad E_{\gamma_2} \le 3.64e^{-\pi m(Q_{2,3,4})} + 5.26e^{-2\pi m(Q_2)}, \tag{3.30}$$

provided $m(Q_2) \ge 1.5$. This emerges from (2.36), (2.37), (3.11), (3.25) and the triangle inequalities

$$E_{\gamma_1} \le \max_{z\in\gamma_1} |f(z) - f_{1,2,3}(z)| + \max_{z\in\gamma_1} |f_{1,2,3}(z) - f_{1,2}(z)|, \tag{3.31}$$

$$E_{\gamma_2} \le \max_{z\in\gamma_2} |f(z) - f_{2,3,4}(z)| + \max_{z\in\gamma_2} |f_{2,3,4}(z) - f_{3,4}(z) - i\varepsilon_m| + \varepsilon_m, \tag{3.32}$$

because $m(Q_{2,3}) = 2m(Q_2)$.

(iii) Since $m(Q_{1,2,3}) \ge 2m(Q_2)$ and $m(Q_{2,3,4}) \ge 2m(Q_2)$, it follows from (3.30) that the DDM errors on the boundary segments γ_1, γ_2 satisfy

$$E_{\gamma_j} = \mathcal{O}(e^{-2\pi m(Q_2)}), \quad j = 1, 2. \tag{3.33}$$

This should be compared with the order of the DDM errors on the crosscut of decomposition l, i.e.

$$E_l^{\{j\}} = \mathcal{O}(e^{-\pi m(Q_2)}), \quad j = 1, 2, \tag{3.34}$$

and with the order of the error of the DDM approximation for the conformal module, i.e.

$$\varepsilon_m = m(Q) - \{m(Q_{1,2}) + m(Q_{3,4})\} = \mathcal{O}(e^{-2\pi m(Q_2)}) \tag{3.35}$$

(see (3.14) and (3.25)).

(iv) In (3.33) and (3.34) the indicated orders are best possible. For (3.34), this follows from [12, §7], and for (3.33) from the sharpness of the order of the estimate for ε_m (see [6, Thm. 5]), because

$$E_{\gamma_2} \geq |f(z_4) - f_{3,4}(z_4)| = |i\{m(Q) - m(Q_{1,2})\} - im(Q_{3,4})| = \varepsilon_m.$$

4 Numerical examples

In this section we present three numerical examples illustrating the application of the DDM results obtained in Section 3. Our objectives are as follows:

1. To compare the theoretical estimates for the errors given by (3.14) and (3.30) with the actual DDM errors. We do this in Example 4.1, by considering a polygonal domain for which we can find reliable approximations to the various conformal maps involved in the decomposition.

2. To illustrate how the DDM can be used in conjunction with the numerical conformal mapping package SC Toolbox of Driscoll [3], for the efficient computation of the conformal mapping of complicated polygonal quadrilaterals.

3. To present an example where, due to the effects of crowding, the conformal mapping software that we have available can approximate the conformal map only through the use of domain decompositions.

Example 4.1 We consider the decomposition illustrated in Figure 4.1 and compute approximations to the three conformal maps $f : \Omega \to R_{m(Q)}$, $f_{1,2} : \Omega_{1,2} \to R_{m(Q_{1,2})}$ and $f_{3,4} : \Omega_{3,4} \to R_{m(Q_{3,4})}$ by means of the conventional

method, i.e., by using the unit disc D as intermediate canonical domain. For this we use: (a) the double precision version of the integral equation conformal mapping package CONFPACK of Hough [10]† to compute the conformal map of the defining domain of each quadrilateral onto the unit disc; (b) the subroutine WSC of the Schwarz-Christoffel package SCPACK of Trefethen [21], [20] to compute the inverse Jacobian elliptic sine that takes D onto the associated rectangle.

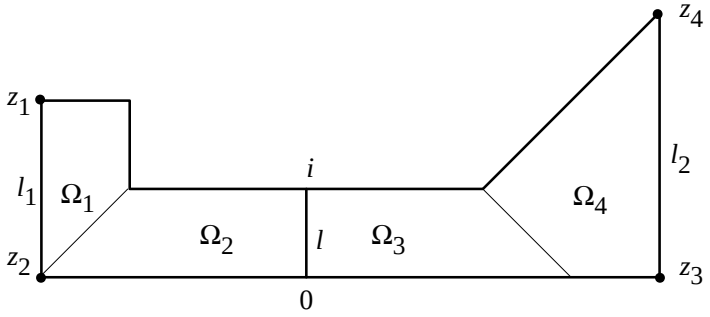

Figure 4.1 The coordinates of the special points, starting from z_1 and moving in counterclockwise order, are (-k-1.,2.), (-k-1.,0.), (k+2.,0.), (k+2.,3.)

Regarding accuracy, we expect that the computed approximations to the functions f, $f_{1,2}$ and $f_{3,4}$, (and to the associated conformal modules $m(Q)$, $m(Q_{1,2})$ and $m(Q_{3,4})$) are correct to at least 8 decimal places. This is so because (see e.g. [4, p. 188]):

- the CONFPACK error estimates for the conformal maps onto the unit disc are less than 1.0×10^{-12};
- in the worst case, the measure of crowding is 6.4×10^{-4}. (This occurs in the computation of $f : \Omega \to R_{m(Q)}$ corresponding to the value $k = 2$.)

In presenting the numerical results, we employ the following notations:

†The double precision version of CONFPACK has only become available recently; see `http://www.mis.coventry.ac.uk/~dhough/`

- $E_l^{\{j\}}$ and E_{γ_j}, $j = 1, 2$: These denote the "actual" DDM errors (3.28)–(3.29):

$$E_{\gamma_1} := \max_{z \in \gamma_1} |f(z) - f_{1,2}(z)|, \quad E_l^{\{1\}} := \max_{z \in l} |f(z) - f_{1,2}(z)|$$

and

$$E_{\gamma_2} := \max_{z \in \gamma_2} |f(z) - f_{3,4}(z)|, \quad E_l^{\{2\}} := \max_{z \in l} |f(z) - f_{3,4}(z)|.$$

The above errors are determined by using the computed (accurate) approximations to the mapping functions f, $f_{1,2}$ and $f_{3,4}$, and then sampling the error functions $f(z) - f_{1,2}(z)$ and $f(z) - f_{3,4}(z)$ at an appropriate number of test points.

- $T(E_l^{\{j\}})$ and $T(E_{\gamma_j})$, $j = 1, 2$: These denote respectively the theoretical estimates for the errors $E_l^{\{j\}}$ and E_{γ_j} given by Theorem 3.2 and Remark 3.2(ii), i.e.

$$T(E_l^{\{j\}}) := 6.17e^{-\pi m(Q_2)}, \quad j = 1, 2 \tag{4.1}$$

and

$$T(E_{\gamma_1}) := 3.64e^{-\pi m(Q_{1,2,3})}, \quad T(E_{\gamma_2}) := 3.64e^{-\pi m(Q_{2,3,4})} + 2.56e^{-2\pi m(Q_2)}. \tag{4.2}$$

- $\delta(E_l^{\{j\}})$ and $\delta(E_{\gamma_j})$, $j = 1, 2$: These denote the values used for testing the validity of the predicted orders of the errors (4.1) and (4.2). They are determined from the computed values of the errors $E_l^{\{j\}}$ and E_{γ_j}, $j = 1, 2$, by: (a) assuming that

$$E(k) \approx Ce^{-\delta \pi m(k)},$$

where $E(k)$ stands for any of the errors $E_l^{\{j\}}$, E_{γ_j} corresponding to the parameter k, δ denotes the associated order $\delta(E_l^{\{j\}})$ or $\delta(E_{\gamma_j})$, and $m(k)$ is the conformal module $m(Q_2)$ corresponding to the parameter k; (b) computing the various values of δ by means of the formula

$$\delta = -\{\log[E(k_1)/E(k_2)]\}/\{\pi(m(k_1) - m(k_2))\},$$

where k_1 and k_2 are taken to be successive values of the parameter k for which numerical results are listed. (Therefore, from the theory we expect to obtain values $\delta(E_l^{\{j\}}) \approx 1$ and $\delta(E_{\gamma_j}) \approx 2$, $j = 1, 2$; see (3.34) and (3.33).)

The numerical results corresponding to the values $k = 1.00(0.25)\ 2.00$ are listed in Tables 4.1, 4.2 and 4.3

k	$m(Q_2)$	$m(Q_{1,2,3})$	$m(Q_{2,3,4})$
1.00	1.279 261 571	3.011 339 975	3.580 314 205
1.25	1.529 343 036	3.511 418 501	4.080 380 645
1.50	1.779 359 959	4.011 434 815	4.580 394 449
1.75	2.029 363 476	4.511 438 206	5.080 397 319
2.00	2.229 364 207	5.511 438 911	5.580 397 915

Table 4.1: Auxiliary conformal modules

k	$E_l^{\{1\}}$	$T(E_l^{\{1\}})$	$\delta(E_l^{\{1\}})$	E_{γ_1}	$T(E_{\gamma_1})$	$\delta(E_{\gamma_1})$
1.00	4.3e-4	*	-	3.7e-6	*	-
1.25	1.9e-4	5.0e-2	1.01	7.6e-7	5.8e-5	2.00
1.50	8.8e-5	2.3e-2	1.00	1.6e-7	1.2e-5	2.00
1.75	4.0e-5	1.0e-2	1.00	3.3e-8	2.5e-6	2.00
2.00	1.8e-5	5.6e-3	1.00	6.9e-9	5.3e-7	2.00

Table 4.2: Errors and orders in the approximation to f by $f_{1,2}$

More precisely, Table 4.1 contains the values of the auxiliary conformal modules $m(Q_2)$, $m(Q_{1,2,3})$ and $m(Q_{2,3,4})$ that are needed in order to perform the DDM error analysis; see Theorem 3.2 and (4.1)–(4.2). They were computed by means of the subroutine RESIST of SCPACK and are expected to be correct to all the figures quoted.

Example 4.2 Consider the quadrilateral $Q := \{\Omega; z_1, z_2, z_3, z_4\}$ of Figure 4.2, where the width of each strip of the spiral Ω is 1, and the special points z_1,

k	$E_l^{\{2\}}$	$T(E_l^{\{2\}})$	$\delta(E_l^{\{2\}})$	E_{γ_2}	$T(E_{\gamma_2})$	$\delta(E_{\gamma_2})$
1.00	4.3e-4	*	-	8.3e-7	*	-
1.25	1.9e-4	5.0e-2	1.01	1.7e-7	1.8e-4	2.00
1.50	8.8e-5	2.3e-2	1.00	3.6e-8	3.8e-5	2.00
1.75	4.0e-5	1.0e-2	1.00	1.2e-8	7.8e-6	**
2.00	1.8e-5	5.6e-3	1.00	1.2e-8	2.6e-6	**

Table 4.3: Errors and orders in the approximation to f by $f_{3,4}$

z_2, z_3, z_4, of Q are, respectively, the four (outermost and innermost) corners $19+18i$, $18+18i$, $9+9i$, $10+9i$ of Ω. The above quadrilateral was first considered in [11], for the purpose of illustrating the performance of a modified Schwarz-Christoffel technique for the mapping of elongated quadrilaterals, and in the sequel in [16] and [18], as a case of application of the DDM for conformal modules, where, in in particular the estimate

$$132.704\ 5393 < m(Q) < 132.704\ 5393$$

was obtained (see [18, pp. 276–277]). Here, we recall it in order to demonstrate the gain in computational time, when using domain decomposition. We do this by means of the MATLAB Schwarz-Christoffel (SC) Toolbox of Driscoll [3] as follows: We call the subroutine `rectmap` of the SC Toolbox, to construct approximations to the associated conformal maps $f : \Omega \to R_{m(Q)}$ and $f_j : \Omega_j \to R_{m(Q_j)}$, $j = 1, 2, \ldots, 10$, and report, for each case the elapsed CPU time. We note, in passing, that the particular subroutine of the Toolbox circumvents the crowding difficulties, by employing the cross ratio and Delanay triangulation technique of Driscoll and Vavasis [2], and for this reason introduces a number of additional vertices on the on the sides of the defining polygon.

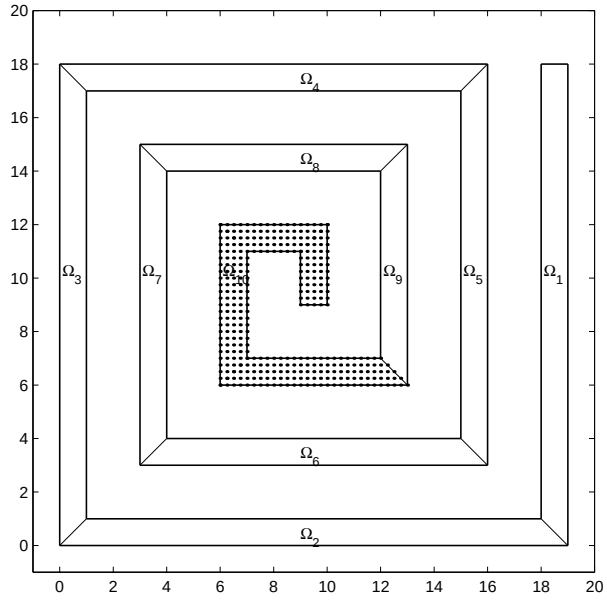

Figure 4.2 The decomposition of Q and the grid points on $\overline{\Omega}_{10}$

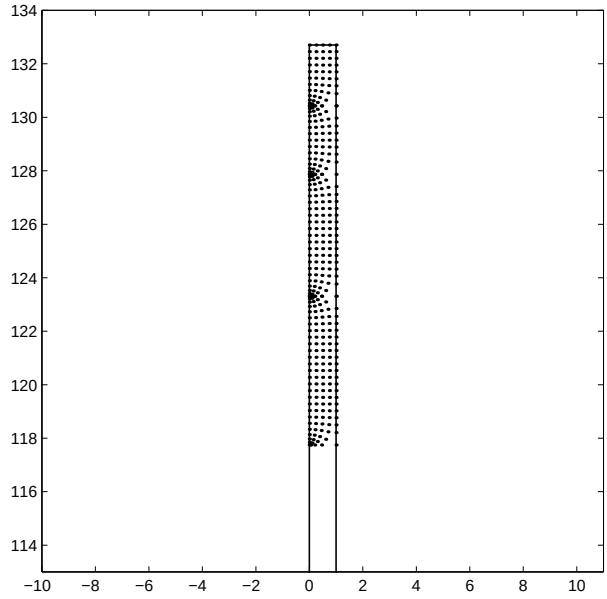

Figure 4.3 The images of the grid points on the (partly shown) conformally equivalent rectangle

The numerical results for the quadrilaterals Q and Q_j, $j = 1, 2, \ldots, 10$ are contained in Table 4.4, where we use the following notations:

- Time I: this denotes the CPU time, in seconds, that are needed for the setting up of the mapping function.
- Time II: this denotes the CPU time, in seconds, required for the mapping of a 0.25×0.25 grid on the polygon onto the associated rectangle.
- N: This denotes the total number of vertices introduced by the Toolbox.
- $\widetilde{m}$: This denotes the estimate of the conformal module provided by Toolbox.

	N	time I	time II	$\widetilde{m}$
Q	136	12686	447	132.704 540
Q_1	20	69	29	17.279 364
Q_2	20	68	29	17.558 279
Q_3	20	70	26	16.558 279
Q_4	20	58	23	14.558 279
Q_5	20	55	21	13.558 279
Q_6	14	70	20	11.558 279
Q_7	8	49	26	10.558 279
Q_8	8	28	19	8.558 279
Q_9	8	23	15	7.558 279
Q_{10}	16	100	35	14.955 345

Table 4.4:

In all the computations the apparent accuracy estimate produced by the Toolbox was less than 3.0×10^{-7}.

All the computations were made using MATLAB 5.3, on an IBM RS 6000/360 workstation.

We end this section by presenting one example that involve quadrilaterals for which the software that we have available can approximate the corresponding conformal map only through the use of DDM.

Example 4.3 Consider the quadrilateral $Q := \{\Omega; z_1, z_2, z_3, z_4\}$ of Figure 4.4,

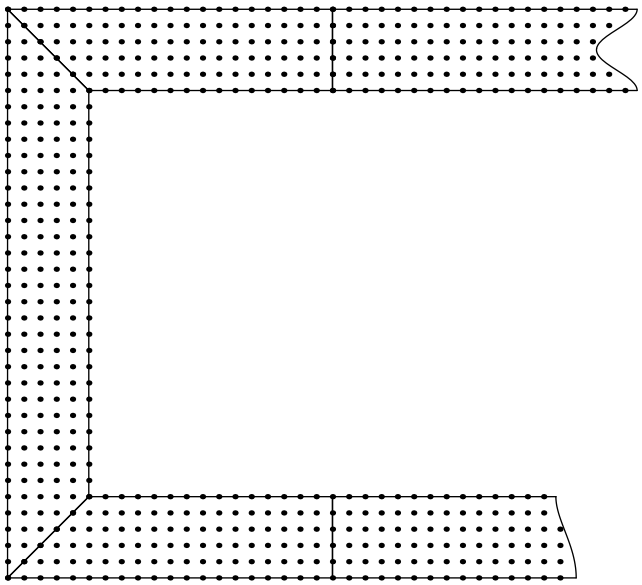

Figure 4.4 The decomposition of Q and the grid points on $\overline{\Omega}$

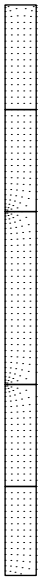

Figure 4.5 The images of the grid points on the conformally equivalent rectangle

References

[1] L. V. Ahlfors, *Conformal Invariants: Topics in geometric function theory*, McGraw-Hill, New York, 1973.

[2] T. A. Driscol and S. A. Vavasis, *Numerical conformal mapping using cross-ratios and Delaunay triangulations.* SIAM, J. Sci. Comput. (in press).

[3] T. A. Driscoll, *A MATLAB Toolbox for Schwarz-Christoffel mapping*, ACM Trans. Math. Soft., 22 (1996), pp. 168–186.

[4] M. I. Falcão, N. Papamichael, and N. S. Stylianopoulos, *Curvilinear crosscuts of subdivision for a domain decomposition method in numerical conformal mapping*, J. Comput. Appl. Math., 106 (1999), pp. 177–196.

[5] D. Gaier and W. K. Hayman, *Moduli of long quadrilaterals and thick ring domains*, Rend. Mat. Appl., 10 (1990), pp. 809–834.

[6] ——, *On the computation of modules of long quadrilaterals*, Constr. Approx., 7 (1991), pp. 453–467.

[7] D. Gaier and N. Papamichael, *On the comparison of two numerical methods for conformal mapping*, IMA J. Numer. Anal., 7 (1987), pp. 261–282.

[8] W. K. Hayman, *Remarks on Ahlfors' distortion theorem*, Quart. J. Math. (Oxford), 19 (1948), pp. 33–53.

[9] P. Henrici, *Applied and Computational Complex Analysis*, vol. III, Wiley, New York, 1986.

[10] D. M. Hough, *User's Guide to CONFPACK*, IPS Research Report 90-11, ETH-Zentrum, CH-8092 Zurich, Switzerland, 1990.

[11] L. H. Howell and L. N. Trefethen, *A modified Schwarz-Christoffel transformation for elongated regions*, SIAM J. Sci. Stat. Comput., 11 (1990), pp. 928–949.

[12] R. Laugesen, *Conformal mapping of long quadrilaterals and thick doubly connected domains*, Constr. Approx., 10 (1994), pp. 523–554.

[13] N. Papamichael, *Numerical conformal mapping onto a rectangle with applications to the solution of Laplacian problems*, J. Comput. Appl. Math., 28 (1989), pp. 63–83.

[14] N. Papamichael and N. S. Stylianopoulos, *On the numerical performance of a domain decomposition method for conformal mapping*, in Computational methods and function theory 1989, St. Ruscheweyh, E. B. Saff, L. C. Salinas, and R. S. Varga, eds., vol. 1435 of Lecture Notes in Math., Springer, Berlin, 1990, pp. 155–169.

[15] ——, *A domain decomposition method for conformal mapping onto a rectangle*, Constr. Approx., 7 (1991), pp. 349–379.

[16] ——, *A domain decomposition method for approximating the conformal modules of long quadrilaterals*, Numer. Math., 62 (1992), pp. 213–234.

[17] ——, *On the theory and application of a domain decomposition method for computing conformal modules*, J. Comput. Appl. Math., 50 (1994), pp. 33–50.

[18] ——, *Domain decomposition for conformal maps*, in Computational methods and function theory 1994, R. M. Ali, St. Ruscheweyh, and E. B. Saff, eds., vol. 5 of Ser. Approx. Decompos., World Sci. Publishing, River Edge, NJ, 1995, pp. 267–291.

[19] ——, *The asymptotic behavior of conformal modules of quadrilaterals with applications to the estimation of resistance values*, Constr. Approx., 15 (1999), pp. 109–134.

[20] L. N. Trefethen, *Numerical computation of the Schwarz-Christoffel transformation*, S.I.A.M. J. Sci. Stat. Comput., 1 (1980), pp. 82–102.

[21] ——, *SCPACK User's Guide*, Numerical Analysis Report 89-2, Dept of Maths, MIT, Cambridge, MA, 1989.

M.I. Falcão,
Centro de Matemática,
Universidade do Minho,
Campus de Gualtar,
4700 Braga, Portugal,
e-mail: mif@math.uminho.pt

N. Papamichael,
Department of Mathematics and Statistics,
University of Cyprus,
P.O. Box 20537, CY-1678 Nicosia, Cyprus.
e-mail: nickp@ucy.ac.cy

N.S. Stylianopoulos,
Department of Mathematics and Statistics,
University of Cyprus,
P.O. Box 20537, CY-1678 Nicosia, Cyprus.
e-mail: nikos@ucy.ac.cy